Ground Support 2026 - D Cumming-Potvin & J Wesseloo (eds.)
© 2026 Australian Centre for Geomechanics, Perth
doi:10.36487/ACG_repo/2625_22

Managing challenging ground conditions: a Cuiabá Mine case study on utilising rapid automated deformation tracking for ground support optimisation

Jochen Franke [b,*], Bruna de Almeida Pires Souza [c], Marcelo Pereira Campos [a], Jih Horng Liu [c], Carlos Gonzalez [b]

[a] *AngloGold Ashanti, Brazil*

[b] *Caroni Geospatial Pty Ltd, Australia*

[c] *Cuiabá Mine, AngloGold Ashanti, Brazil*

Abstract

AngloGold Ashanti operates a number of underground mines in different regions, including Cuiabá Mine in the Mineração complex in Brazil. Cuiabá is a significant gold producer in Brazil and one of the company's key assets in the Americas. Its underground operation is known for its rheology contrast across banded iron formation, Meta-Adesites, requiring advanced safety measures for mining and environmental control. With depth come increased challenges, including geotechnical ground conditions as laid out in its paper. Cuiabá operational team have a long-standing tradition and many success stories of adopting cutting-edge technologies to manage such challenges.

This paper details how one such technology of utilising automated ground support tracking of in situ rockbolts on the basis of LiDAR scan cloud collection is applied to not only identify deterioration in ground support, but also to accurately determine its remaining capacity. A case study based on dense spatial and temporal data from rapidly collected scans within days of each other tracked a severe deformation in high detail. This was only possible because of the high degree of automation of the system in use, which eliminated the need for personnel to process any of the raw data, and allowed for thorough and timely geotechnical analysis instead.

One of the case study outcomes as detailed in the paper was the ability to better define representative in situ rockbolt capacities than what is possible to estimate with laboratory or pull testing of ground support elements in isolation. Such remaining in situ ground support capacity data can then be used as quantified inputs into preventative and therefore safer rehabilitation planning for other areas with the same ground support in use.

Keywords: *LiDAR, deformation/convergence monitoring, instrumentation and monitoring, automated point cloud processing, ground support optimisation, determining ground support capacity, ground support rehabilitation*

1 Introduction

1.1 Cuiabá Mine

The Cuiabá Mine is located in the municipality of Sabará, in the northwestern sector of the Quadrilátero Ferrífero, within the central region of Minas Gerais, Brazil. This underground gold operation, owned by AngloGold Ashanti, currently extends to depths of approximately 1,600 m and employs the sublevel stoping mining method. Due to its considerable depth, it is recognised as one of the deepest operating mines in Brazil.

[*] Corresponding author. Email address: jochen.franke@caroni.com.au

The Cuiabá gold deposit forms part of the Archean–Proterozoic (Au, Fe, Mn) metallogenic province of the Quadrilátero Ferrífero, located along the southern margin of the São Francisco Craton (SFC). This deposit represents a world-class example of orogenic gold mineralisation and is hosted within the Rio das Velhas Greenstone Belt. The geological framework is characterised by a typical association of mafic to ultramafic volcanic rocks, banded iron formations (BIFs), and carbonaceous and micaceous phyllites, all metamorphosed under greenschist facies conditions. The predominant sulphide mineralisation is hosted within the Archean Cuiabá BIF and is commonly associated with zones of hydrothermal alteration. In addition to the main ore bodies, 3 other styles of mineralisation have been identified, although they have not yet been economically exploited:

- shear zone-related quartz veins
- disseminated sulphides within iron-rich lithologies
- shear-related quartz–carbonate veins.

The deposit comprises metavolcanic and metasedimentary sequences displaying mineral assemblages typical of greenschist facies metamorphism. As illustrated in Figure 1, the local lithostratigraphic framework includes, at the base, a lower metamafic unit (MAN), subdivided into proximal (X2), intermediate (X2CL), and distal (MANX) hydrothermal alteration zones. This unit is overlain by BIFs and metachert units (carbonate, carbonaceous, and ferruginous), followed by carbonaceous phyllites (XG). The sequence continues with an upper metamafic unit (MBA), also subdivided into proximal (X2), intermediate (X2CL), and distal (MBAX) alteration zones. The uppermost portion of the stratigraphic column consists of metavolcanoclastic rocks (XS) and micaceous phyllites (X1) (Rodrigues et al. 2007).

According to Fernandes et al. (2016), the structural architecture of the deposit reflects the superposition of three main deformational phases, each associated with distinct structural features and mineralisation events. The first phase (D1) is characterised by inclined, tight folds with axes plunging toward the ESE, accompanied by the development of S1 foliation and gold mineralisation associated with deformed pyrrhotite. The second phase (D2) comprises tight, inclined folds that are coaxial with those of D1, also plunging to the ESE, and is associated with the development of S2 foliation. Gold mineralisation during this phase is primarily related to subhedral pyrite occurring within quartz–carbonate veinlets parallel to the axial planes of these folds. The third phase (D3) is characterised by the development of gentle folds with sub-horizontal axes and vergence toward the west, as well as a spaced crenulation cleavage trending north-south. This phase locally overprints and segments structures formed during the earlier deformation events.

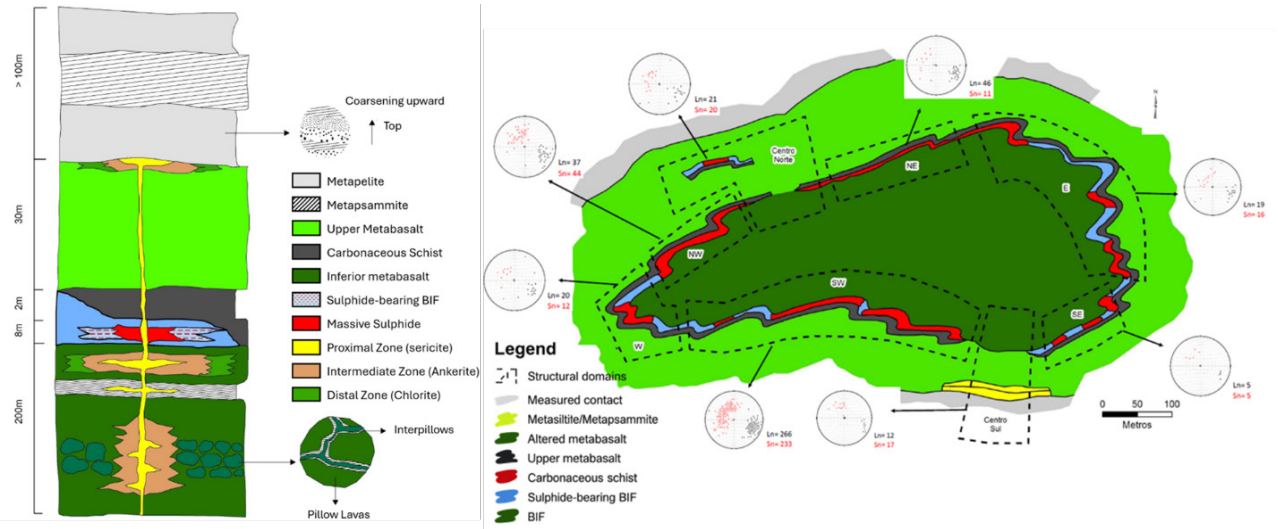


Figure 1 Lithostratigraphic column of the Cuiabá deposit, including associated hydrothermal alteration zones, and geological map of the deposit showing structural domains and corresponding stereographic projections. Ln = fold axes related to D1/D2 phases; Sn = pole to S1/S2 foliation (modified from Fernandes et al. 2016)

1.2 Site ground support

The evolution of the ground support system at the Cuiabá Mine is intrinsically linked to the progressive increase in mining depth and the resulting intensification of the in situ stress field. Prior to 2019, support design was primarily based on reinforcement using rebar bolts, focusing on localised stability control of backs and walls. At this stage, the support philosophy was largely driven by structurally controlled instability, with limited consideration of stress-induced failure mechanisms. The subsequent incorporation of shotcrete represented an initial shift toward surface confinement, improving load distribution and enhancing the global response of the excavation-support system.

As mining advanced to greater depths, the rock mass response became increasingly governed by stress-driven mechanisms, including yielding and time-dependent deformation. The initial manifestation of squeezing conditions marked a critical transition, requiring a reassessment of both support capacity and deformability. In response, the support systems evolved toward integrated solutions combining fibre-reinforced shotcrete applied after each blast, systematic mesh installation, and the adoption of higher-capacity and more ductile reinforcement systems, designed to better accommodate increasing deformation demand and enhance support performance under squeezing conditions. Furthermore, the introduction of cable bolts in large-span excavations to provide deeper anchorage.

In the most recent and deeper mining stages, where squeezing conditions have become more pronounced and widespread, the support design has evolved into a highly engineered, performance-driven approach. Current systems incorporate multiple complementary elements – yielding bolts, shotcrete, mesh, and cable bolts – aimed at optimising both confinement and energy absorption capacity. The increased support density reflects a more refined understanding of excavation-scale response and geomechanical domains. The design philosophy has thus transitioned toward a convergence control framework, in which support systems are tailored to balance deformation demand and support capacity, ensuring long-term excavation stability under high-stress conditions.

1.3 Squeezing conditions

Geomechanical conditions at the Cuiabá Mine are strongly influenced by structural complexity, lithological variability, and increasing stress levels associated with mining at depth. Major geological discontinuities, including faults, shear zones, and fold-related structures, play a key role in affecting deformation patterns and excavation stability. In particular, shear zones and foliation-parallel weaknesses act as preferential planes for strain localisation, contributing to the development of non-uniform deformation, stress redistribution, and damage to the surrounding rock mass and installed support systems. The interaction between these structural features and the high in situ stress field significantly increases the susceptibility to instability, especially in highly deformed and altered zones.

As mining progresses to greater depths, the rock mass exhibits increasingly severe stress-induced behaviour, with squeezing conditions becoming a dominant challenge in several areas of the mine. The severity of squeezing ranges from moderate to intense, depending on lithology, structural fabric, and excavation geometry. Observed behaviour includes time-dependent convergence, progressive closure of excavations, and deformation-driven damage to support elements such as shotcrete cracking, mesh distortion, and yielding or failure of reinforcement. These conditions require support systems capable of accommodating large deformations while maintaining load-bearing capacity, reinforcing the need for yielding support strategies and convergence-based design approaches.

In addition to squeezing, the mine is subjected to seismic loading associated with stress redistribution at depth and mining-induced rock mass response. Seismic events, ranging from low-magnitude microseismicity to higher-energy events, have been recorded and, in some cases, have resulted in damage to excavations and installed support. Challenging ground conditions are particularly evident in areas where unfavourable structural orientations related to the excavation coincide with high-stress concentrations, when development headings occur in highly foliated or altered rock masses. These conditions have led to severe ground behaviour, including excessive deformation, support overstressing, and localised failures, highlighting

the need for continuous refinement of support design and ground control strategies. Figure 2 illustrates a moderate squeezing condition at the mine's deeper levels.

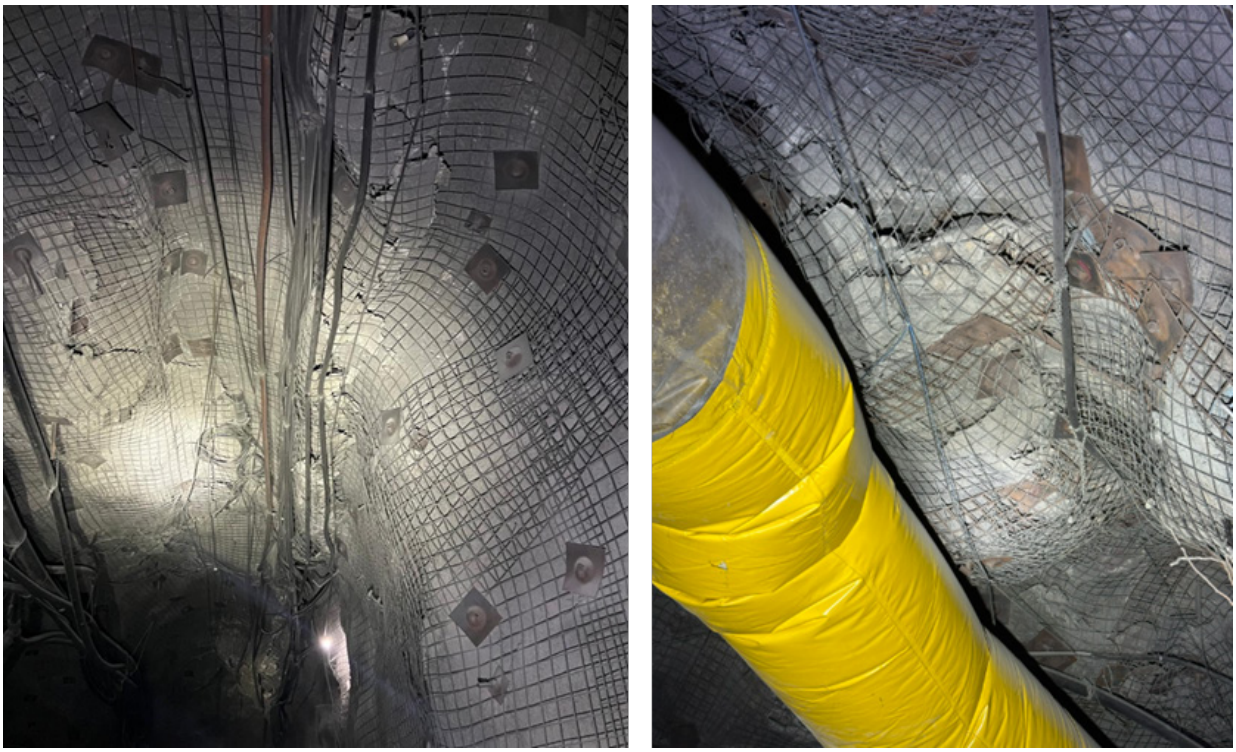


Figure 2 Moderate squeezing-related ground behaviour observed at the 1,550 m depth characterised by pronounced mesh deformation, plate displacement, and localised damage to the shotcrete and reinforcement system

This paper introduces our approach to managing these more challenging conditions through a fully automated LiDAR based monitoring system that allows the site team to track ground support without the overhead of having to invest time, effort, and expertise into the production of associated output data and reporting.

2 Case study

2.1 Level 21 Viana drive

Level 21 (L21) Viana drive was developed as a crosscut and is located in a geotechnically adverse zone of the Cuiabá Mine, where unfavourable rock mass conditions and structural features strongly control excavation behaviour. The rock mass is characterised by low competence and is intersected by a shear zone and influenced by a major geological contact, resulting in a highly fractured rock mass prone to deformation. The most unfavourable rock mass corresponds to the X1 metapelite, which surrounds the L21 Viana drive and exhibits low strength and high deformability. Additionally, the excavation is developed subparallel to the foliation, promoting strain localisation and deformation along existing planes of weakness, which increases susceptibility to stress-induced damage under elevated stress conditions. Figure 3 shows a plan view of the excavations, highlighting the L21 Viana drive and the associated lithological model.

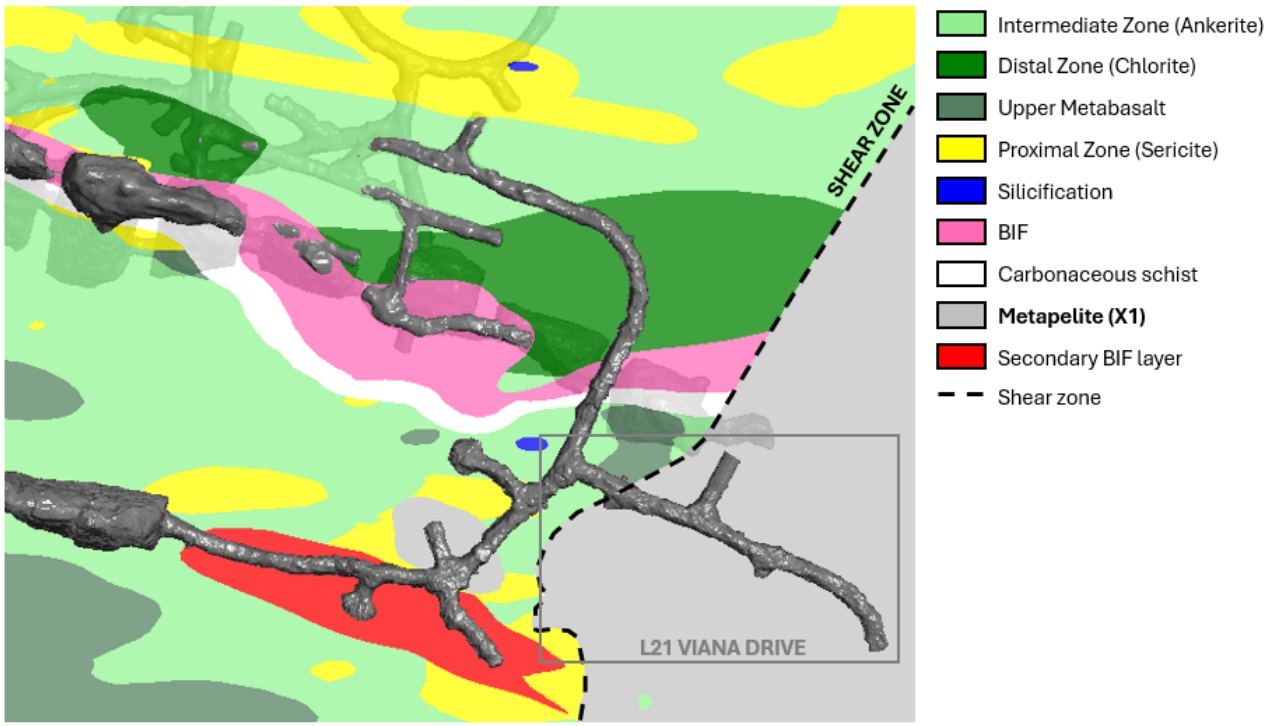


Figure 3 Plan view of the excavations at the Level 21 Viana drive, showing their spatial relationship with lithological units, hydrothermal alteration zones (sericite, ankerite, and chlorite), and the main shear zone

As mining progressed to greater depths, the rock mass response transitioned to a stress-dominated regime, leading to pronounced squeezing behaviour characterised by time-dependent deformation, progressive convergence, and operational impacts such as borehole closure and difficulties during production activities. The increasing deformation demand resulted in load redistribution within the support system, causing mesh damage, plate rotation, and localised overstressing and also some failure of reinforcement elements, indicating that the imposed strain exceeded the initial support capacity. Due to the rapid evolution of deformation and its implications for safety and operability, the area was selected for high-frequency LiDAR monitoring. This approach enabled the quantification of displacement and strain rates, as well as the characterisation of the spatial and temporal evolution of deformation and its correlation within stoping areas.

2.2 VoidMapper system in use for automated deformation tracking

AngloGold Ashanti was looking to address the need for robust and efficient deformation monitoring by deploying proven technology available from a suitable vendor. Unlike point-wise methods such as extensometers that cannot measures along wide areas, 3D LiDAR scanning has been shown to be adequate for tracking swelling or squeezing ground conditions.

Raw 3D LiDAR data collected in underground drives and other voids is, as such, not directly usable for the purpose of deformation tracking. It needs to be processed into a derivative form that lends itself for interpretation and analysis, and ultimately actionable reporting for decision-making to achieve safe and cost-effective outcomes for underground mining operations. The necessary steps involved in this process have been detailed in previous publications (Franke & Gonzalez 2022, 2023, 2024).

Manual LiDAR data processing for geotechnical purposes was originally an obstacle due to the tedious, time-consuming, and error prone nature of the manual workflow from data acquisition to final interpretation. This has since been overcome by the fully automated workflow of the cloud-based software VoidMapper (Franke & Gonzalez 2026), which was designed for the specific underground mining void deformation tracking purpose required by underground geotechnical practitioners. Associated algorithmic

advances addressed systematically false reporting common for third party manual data processing software (Franke & Gonzalez 2024).

2.3 Drive surface deformation monitoring observations

Cuiabá Mine personnel inspected first indications of deformation in the Level 21 Viana Drive in early 2025 and deployed its established LiDAR and VoidMapper tracking system to quantify the process. This sub-chapter provides an overview of scanning frequency (Figure 4) and reported surface deformation (Figure 5).

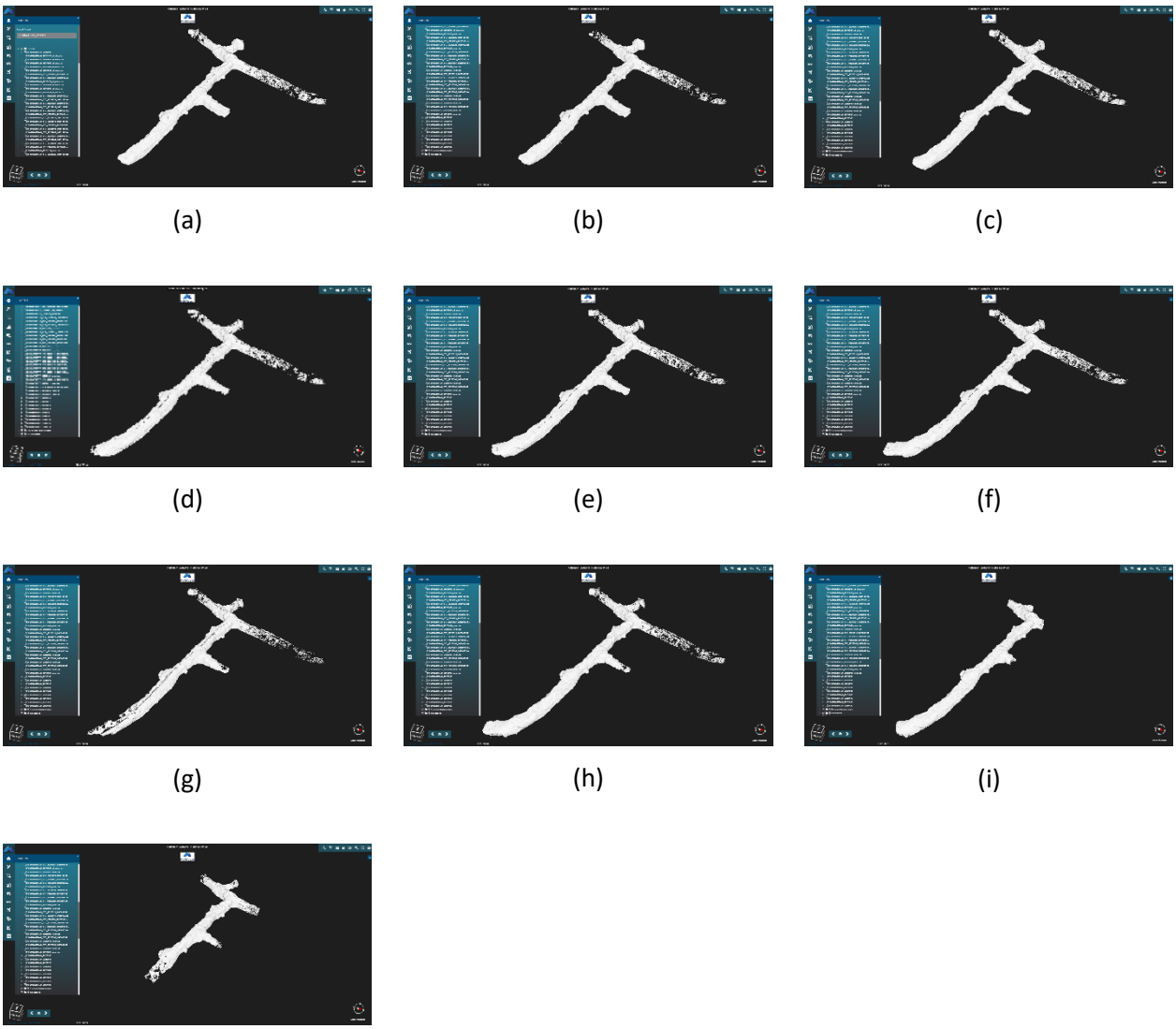


Figure 4 **Overview of coverage and therefore overlap for each LiDAR scan used for drive and rockbolt deformation tracking. Scans were collected at rapid succession commensurate with rapid deformation on (a) 3 September 2025, (b) 9 May 2025, (c) 11 September 2025, (d) 23 September 2025, (e) 26 September 2025, (f) 1 October 2025, (g) 3 October 2025, (h) 10 October 2025, (i) 14 October 2025, and (j) 26 November 2025**

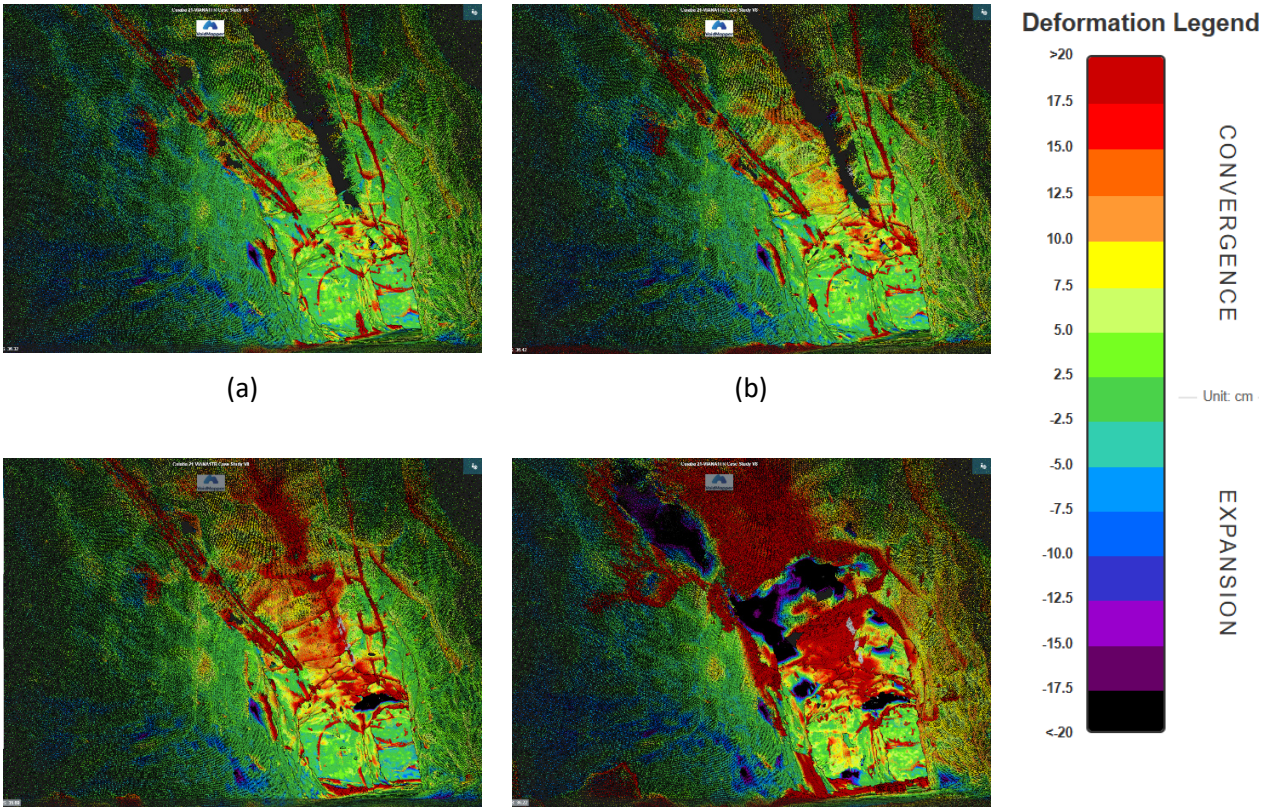
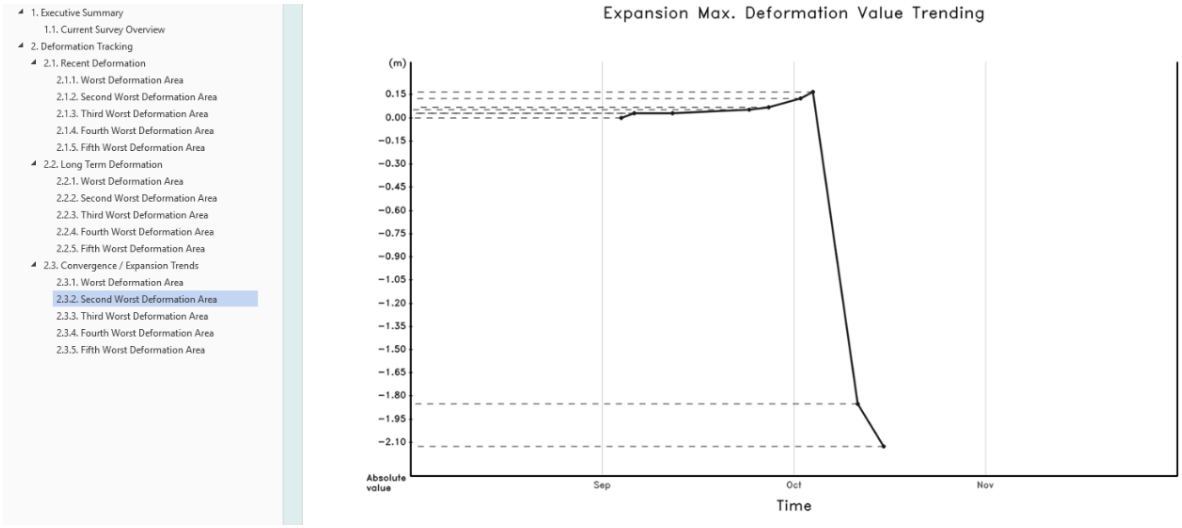


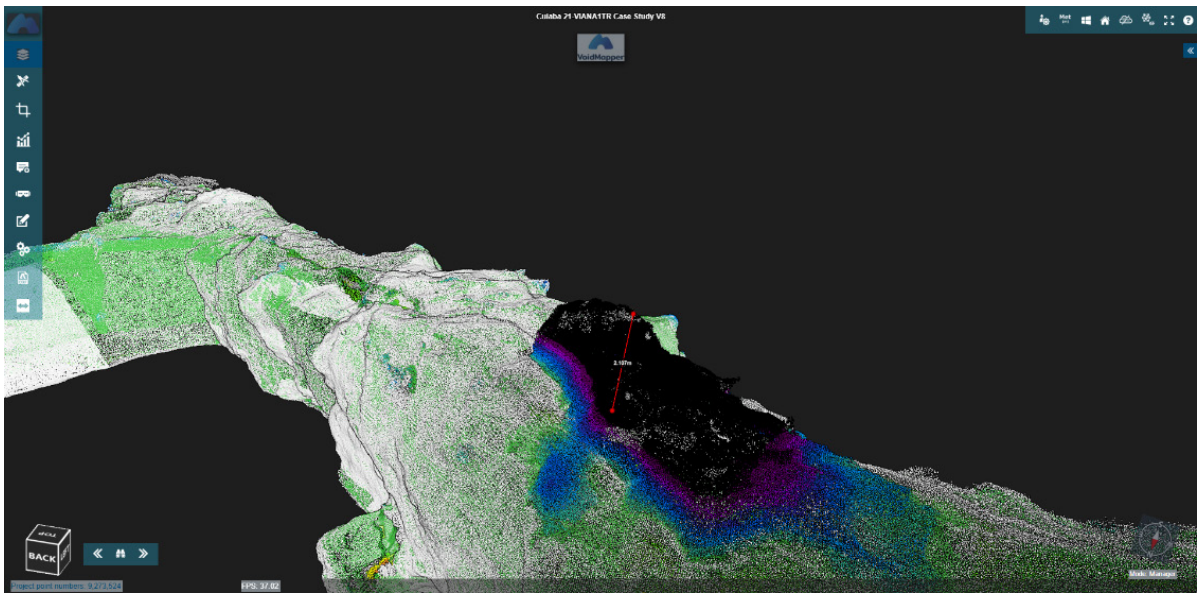
Figure 5 Tracked deformation as per colour legend provided. Yellow, orange and red hues indicate convergence. Blue, purple and black hues indicate expansion, representing rockfalls in this case. Scanning frequency from the baseline date was (a) 20 days, (b) 28 days, (c) 37 days, and (d) 84 days, respectively

As is evident in Figure 5, first rockfalls out of the left sidewall occurred after 20 days of tracking, as shown in blue and purple colours (Figure 5a). Convergence in the backs exceeds 10 cm after 28 days (Figure 5b), and exceeds 15 cm after 37 days, as shown by the progressively darkening orange and red colours. At that same time interval a first notable rock was scaled from the backs, as shown by the localised expansion coloured black towards the end of the drive in Figure 5c. The location of this scaling in the back coincides with the shear zone indicated in Figure 3. After 84 days of tracking, convergence across the entire backs and some sidewall portions of the drive exceeds 20 cm as indicated by the dark red colour, and more scaling was completed in the backs shown as black expansion colour (Figure 5d).

In order to be able to better judge the severity of reported area of scaling, it is informative to provide automatically generated deformation trending data in Figure 6 for the scaled area shown in Figure 5c, as extracted from all automatically generated and reported deformation regions.



(a)



(b)

Figure 6 Automatically generated (a) deformation trending data and (b) 3D outside view for the scaled location shown in Figure 5c. Notably, this area converged around 15 cm within approximately 1 month before falling with a maximum depth of failure of just over 2.1 m

2.4 Rockbolt deformation monitoring observations

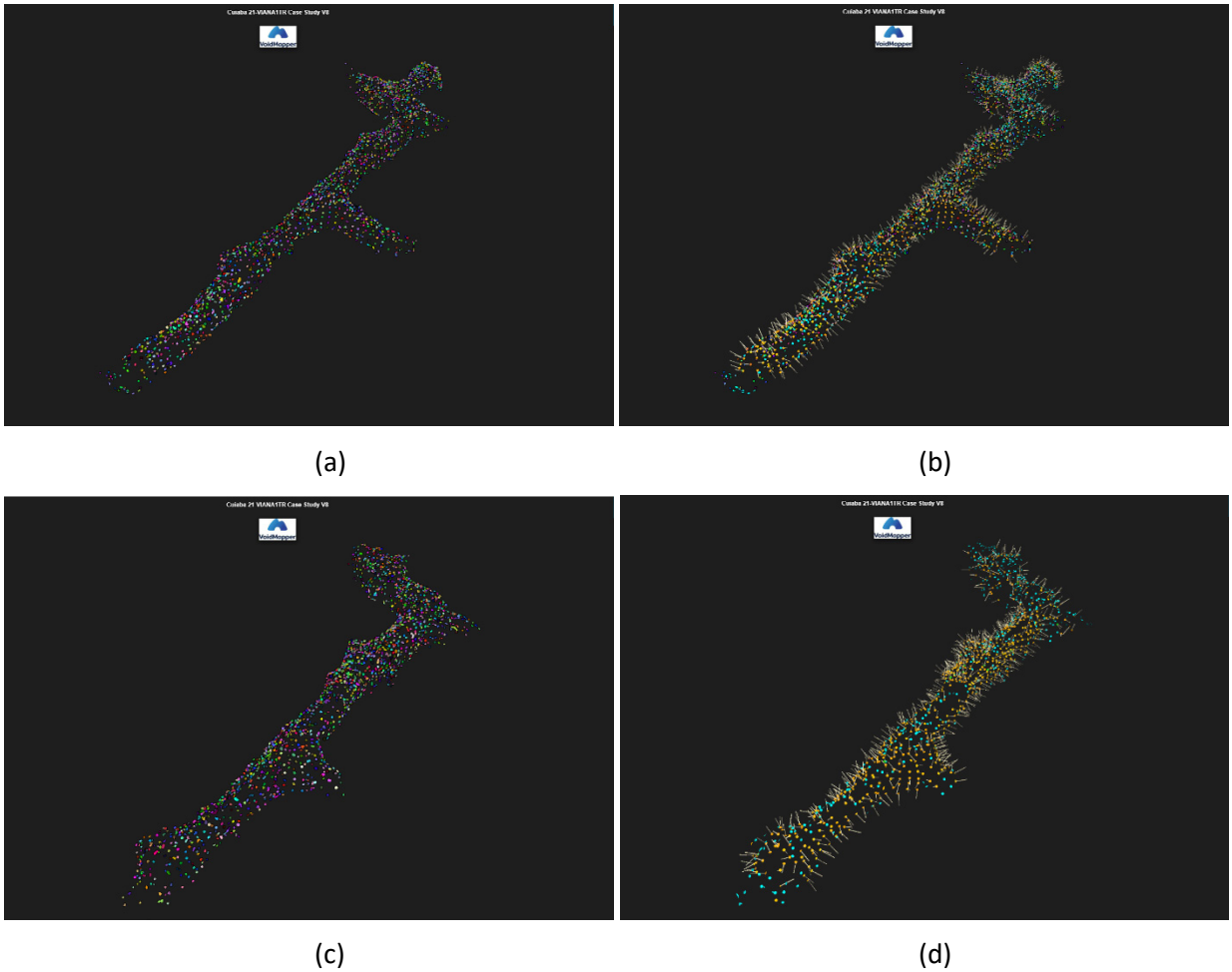
General drive surface deformation data as provided in Section 2.3 is suitable to use as a reference to determine how much installed ground support has deteriorated overall. However, more advanced and refined insights on ground support health can be achieved by isolating from the overall scan cloud and then tracking bolt and plate positions and their deformation over time. Since raw LiDAR scan point clouds don't contain any information on what objects they have captured as a three-dimensional representation within the scene that was scanned, the end user needs to find a way to extract them.

The only practical and effective way to do so is to utilise suitable machine learning (ML) or artificial intelligence (AI) techniques as explained in more detail in Franke & Gonzalez (2023, 2024). This process involves the manual preparation of a suitably large and representative database of rockbolt and plate scan

cloud patches. These data are then used to train a ML or AI algorithm to recognise the characteristics of rockbolts and plates, enabling it to reliably extract these features from any new point cloud presented for classification. In this case, classification is binary, with scan points separated into 2 classes: rockbolts and plates and non-bolt points.

The challenge with such binary classification is to ensure the ML training database contains sufficiently representative and varied samples for both, rockbolts and plates, as well as non-bolts, such that any new scan to automatically classify is appropriately represented. If that is not catered for, then ML classification may result in either too many false positives, or insufficient true positives in the rockbolt and plate class, when considering that the aim is to correctly track the position of ideally all, or at least a sufficiently representative number of rockbolts and plates contained in scan coverage over time. Figure 7 shows that this aim was achieved for the case study as shown for the baseline scan (Figure 7a) and for the last scan of the series (Figure 7c).

Once rockbolts and their plates are isolated as scan patches from the remainder of the scan cloud by ML classification, VoidMapper automatically extracts their respective spatial positions such that these coordinates can be tracked over time by repeating the process for all scans of the series. An overview of this extraction is shown for the baseline scan in Figure 7b, and for the last scan of the series in Figure 7d.



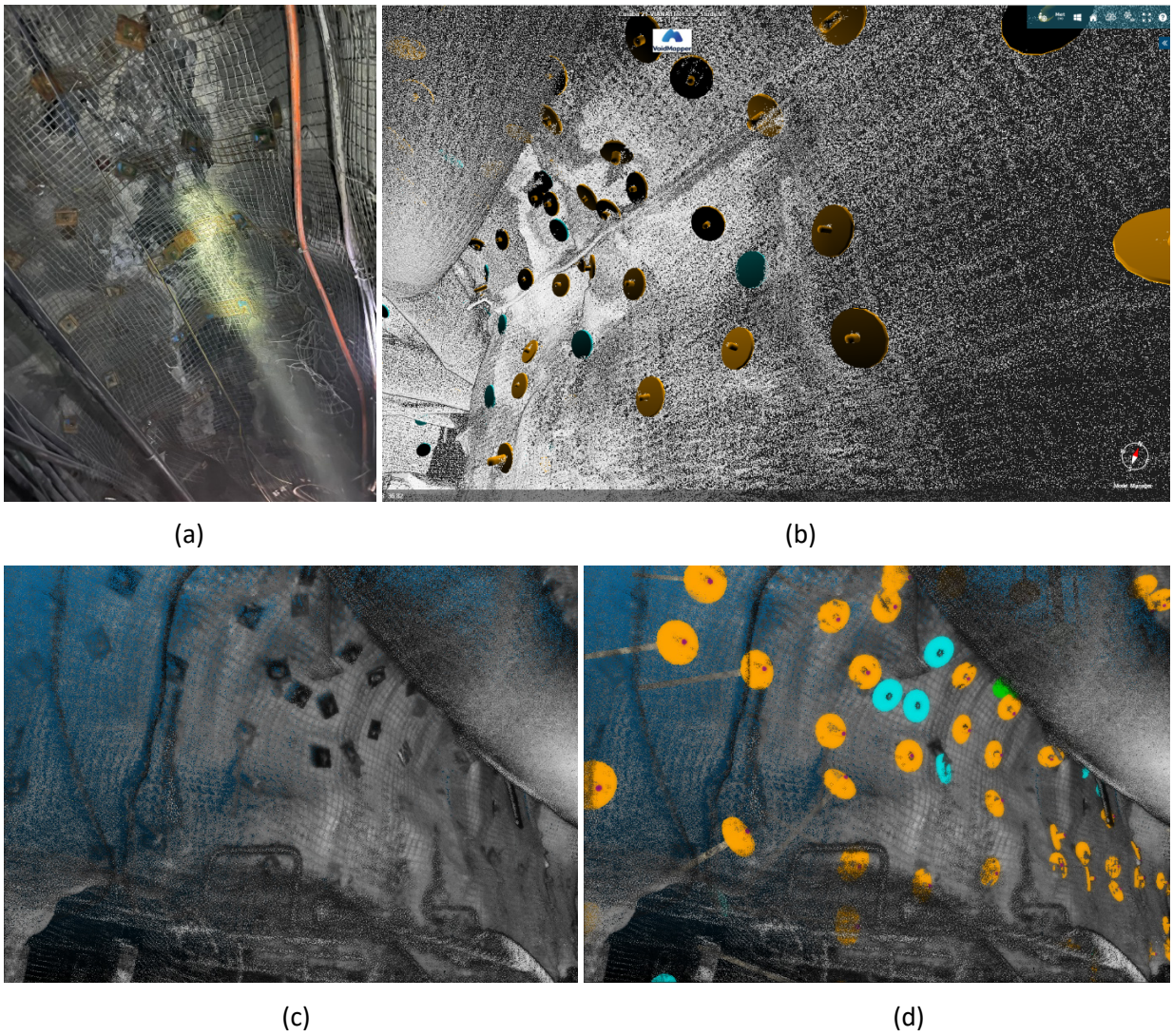
(a) (b)

(c) (d)

Figure 7 Automatically classified rockbolt and plate scan cloud patches using a machine learning (ML)/artificial intelligence (AI) algorithm for the (a) baseline date and (c) the last scan of the series. Extracted rockbolt and plate features using ML/AI classified scan cloud patches for (b) the baseline date (b) and (d) the last scan of the series

Figure 8 shows the output of bolt and plate extraction in more detail, indicating that the precision of bolt and plate tracking is higher than the precision of individual scan points. This improved precision is achieved

because the coordinate extraction process is based on at least dozens of scan points representing each bolt or plate, thereby reducing the influence of individual point errors through statistical averaging.



(a) (b)

(c) (d)

Figure 8 Automatically extracted rockbolts and plate positions based on machine learning (ML)/artificial intelligence (AI) point cloud classification. The photograph (a) shows a typical bolt and plate in situ distribution as extracted by the algorithm and (b) shown as orange bolts and plates, or blue split set plates overlaid over the white scan cloud in. (c) This is a screenshot of a case study 3D scan cloud displayed using intensity values, resembling black and white photography, clearly showing dark plates on lighter walls, and much less clearly other bolts and plates underneath a mesh lower on the wall. (d) Orange and blue bolts and plates extracted for bolt and plate positions and overlaid on the same point cloud and view angle as in (c) indicate the success of the coordinate extraction process for clearly visible as well as less clearly visible bolts and plates

2.5 Preventative rehabilitation considerations

Tracking the position of individual rockbolts and plates over time and the ability to visually interrogate this data in 3D as shown in preceding sections provides insights into ground support behaviour unavailable through other means. Truly meaningful insights become available when such data is aggregated by looking at the combined overall rockbolt and plate deformation behaviour of all tracked bolts and plates in the form of graphs in automatically generated report documents. The ultimate aim is to utilise such reports to plan for preventative rehabilitation rather than being exposed to safety concerns associated with reactive rehabilitation.

Figure 9 shows the overall behaviour of all rockbolts and plates tracked for case study split sets and standard type bolts. Notably, this behaviour is derived from hundreds of bolts extracted for each LiDAR scan, making this data much more representative and reliable than what could be gauged from tracking a low number of single bolts through other deformation tracking methods.

This median deformation graph aggregates automatically extracted rockbolt, and separately plate, position behaviour over time, with each scan date reporting values along the X-axis. The Y-axis on the left reports absolute deformation behaviour represented by thick graph lines, whereas the Y-axis on the right reports deformation rates in metres per month represented by thin lines in the graph. Reported data is further differentiated by bolt type and feature. Orange and red lines represent deformation of standard bolt tip and plate centre – the bolt to plate contact point (BPCP) – respectively. Blue lines represent deformation behaviour of split set plate centres.

There are 2 ways to interrogate absolute deformation behaviour in this graph. Firstly, per individual period in-between scans, which is shown by dotted thick lines. And secondly, cumulatively over time, which is shown by solid thick lines.

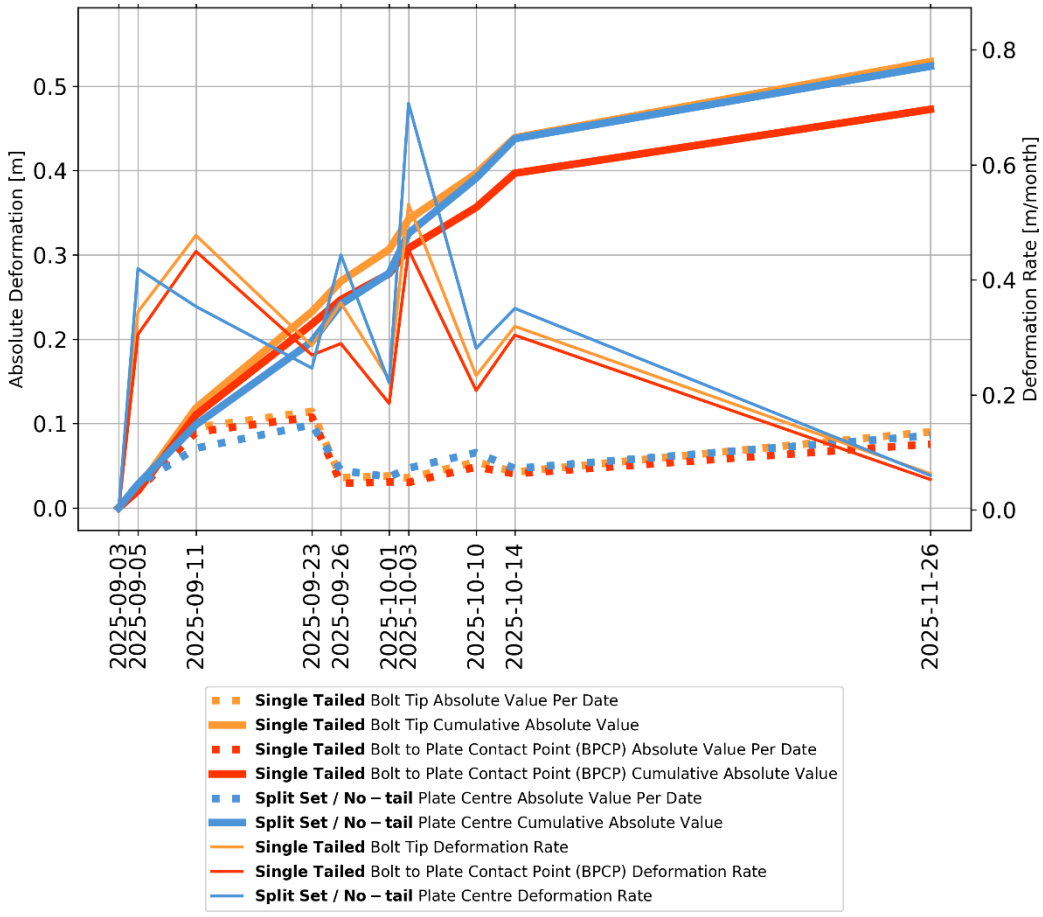


Figure 9 Median deformation of all bolts tracked for the case study as extracted for all 10 scan dates of the series. Thin lines show deformation rate in metres per month on the right Y-axis. Thick lines show absolute deformation in metres on the left Y-axis. Solid thick lines show cumulative absolute deformation over time resulting in a median deformation of nominally 0.5 m over the 84 days of tracking

When interpreting this graph, it is important to account for irregular intervals on the X-axis between values on the graph lines caused by irregular scan dates. Different lines and their values provided in the graph serve different purposes. Spikes in deformation rate indicate times when large deformations dynamics took place, which can help assessing support system capability to absorb dynamic ground behaviour. Solid thick

cumulative deformation lines provide intuitive quantitative confirmation of how much ground support has deformed over time as of the first scan date. If the first available scan was collected sometime after ground support installation, then it may be prudent to allow for deformation that may have occurred before scan tracking commenced.

In this case study, the solid thick lines representing cumulative median deformation for all bolts contained and successfully extracted in the scan area overlap between scan dates indicate that over the course of the first 5.5 weeks standard bolt plates deformed significantly more than for the second 5.5 weeks. One possible explanation for this change in behaviour is that the failing and subsequent scaling of rock in the backs described caused a stress change resulting in reduced deformation.

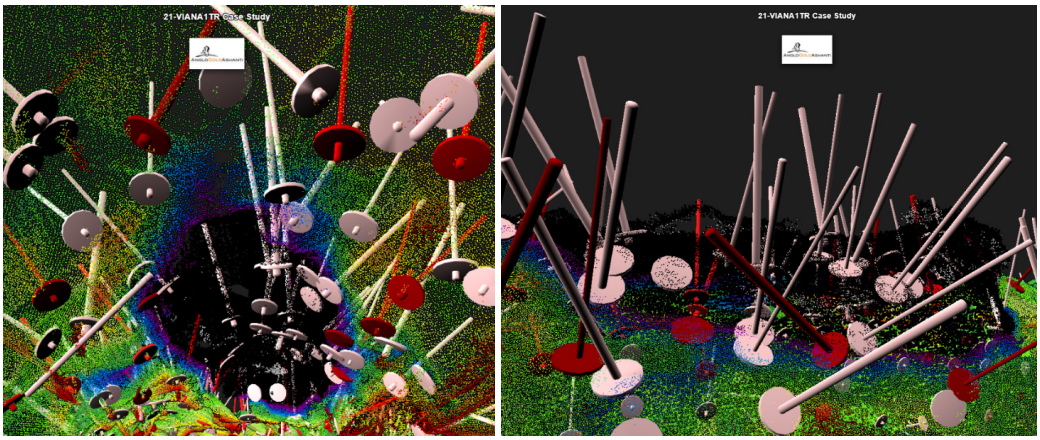
The median deformation graph allows for differentiated assessment of bolt type behaviour, because it provides separate lines for standard bolts and split sets. Since split sets can only be tracked by their plate centre, the best like for like comparison is with standard bolt plate centres. For this case study, it is clear by looking at the thick cumulative absolute deformation lines for standard bolt plates in red, and for split set plates in blue, that split sets have deformed more than standard bolts. This is not unexpected considering that split sets are typically used as an economical but usually less effective part of ground support design. Whether or not the reported behaviour of split sets varies can depend on where exactly in the ground support design they are integrated, and whether that results in more deformation relative to other ground support elements.

Automated tracking of rockbolt deformation produces a number of output files that can be used for different purposes. One of these files is the 3D display of tracked rockbolts and plates coloured by deformation, starting from light pink representing small deformations to dark red representing large deformations. Figure 10 shows the same scaled section of the backs described in Figures 5c and 6 overlaid with extracted rockbolts and plates coloured by deformation. As is evident from this display, original rockbolts installed immediately after excavation of this drive are still visible around the perimeter of the scaled location and have significantly deformed in excess of 40 cm, which probable means the bolt has failed, whereas new rockbolts installed during rehabilitation after scaling into the now exposed surface at the back show very little deformation because they have only just been tracked for a short period of time over their service life.

Recording in situ failure of ground support through this LiDAR based automated tracking series starting from the scan capture of its undeformed state presents a very useful opportunity to have an overall idea of the ground support behaviour. This includes by extension the ground support system as a whole comprising not just individual bolts by type but the combination of different bolt types, as applies to this case study, and their respective plates as the system anchoring features. This assessment, also by extension, accounts for the entire ground support system, which is not active in pull tests. Determining such an in situ rockbolt deformation at failure is a representative measure of system failure limit. Test rigs for combined ground support system testing are emerging as an industry option, but they are not yet in common use, and they have limitations in representing true in situ ground and ground support system installation conditions.

Alternative pull testing of in situ bolts to failure utilises in situ conditions but is also limited by what applicable failure mechanisms can be reproduced in the process. Bolt shearing, for example, cannot be replicated in this way. There are also practical limitations on the amount of pull tests that can realistically be done, making the results prone to sensitive to bolt installation variability and therefore potentially biased. For example, pull resistance may vary significantly between partially and fully resin-grouted bolts.

In situ LiDAR based spatial rockbolt deformation tracking to failure on the other hand has all applicable failure mechanisms naturally accounted for. Tracking hundreds of bolts within all drive areas in the backs and side walls that are subject to varying deformation severity as is evident by the change in deformation colours in Figure 5 also makes it a much more robust process, unbiased by outliers.



(a) (b)

Figure 10 Extracted and tracked rockbolts and plates coloured by deformation severity in shades of red overlaid onto the scan cloud coloured by deformation as described in the legend in Figure 5. Dark red bolts are original bolts installed immediately after drive excavation and have deformed over 40 cm at their location at the edge of and nearby the scaled area coloured black in the scan cloud. Light pink bolts were installed after the scaling during rehabilitation into the newly exposed back and surrounding area. (a) Provides an inside drive view; (b) Provides an outside view illustrating these descriptions

The approach to determining rockbolt and ground support failure limit for the ground support design currently in use is to assess rockbolt deformation at the time of the rehabilitation events described in Figures 5c and 5d. It stands to reason that such ground support failure may also occur in any other mine area using this ground support design that is subject to similar ground conditions as described in Section 2.1. The application of this methodology provides a quantified and robust means to predict support failures in these areas comparable to that of the case study by defining a deformation limit tracked for them to be the trigger for preventative rehabilitation cycles. Since this deformation limit needs to be lower than the one measured at failure for the case study area, the applicable median bolt and plate deformation limit to be used as rehabilitation trigger was defined as 0.3 m.

It is useful to correlate this conservative median bolt and plate deformation limit of 0.3 m as derived from LiDAR deformation to the bolts in use. Cuiabá Mine uses 2 types of bolts in the case study area:

- 3m long friction type bolt with a bar diameter of 20 mm and a vendor specified minimum elongation to failure limit of 15%, which equates to 45 cm. It is complemented by a 6 mm thick 250 × 250 mm combi-plate.
- 3m long resin type bolt with a bar diameter of 20 mm and a resin free area and therefore nominal elongation of 30–40 cm in the collar. The plate specifications are 250 × 250mm and 8 mm thickness.

Vendor supplied elongation to failure limits closely match measured bolt deformation data thickness by the automated LiDAR tracking software system at the time of scaling as indicated in Figure 10. This can be interpreted as in situ ground support system performance leading to similar failure limits as laboratory or pull tests conducted for individual bolt types for this particular case study. There may well be other scenarios and situations where this matching of failure limits between the 2 different methods of determining them does not apply.

The next step in the process of making use of the case study outcome is for Cuiabá to assess in what other similar mine areas the associated 0.3 m median bolt deformation limit could be utilised as a preventative rehabilitation trigger. This will involve correlating comparable ground conditions and installed ground support of a design that is the same or similar to that of the case study.

2.6 Opportunities for ground support design improvement

As detailed in Section 2.5, LiDAR-based rockbolt and plate deformation tracking provides the ability to determine a trigger for preventative rehabilitation to be effective such that the risk of rockfalls can be mitigated. As a next phase, Cuiabá's and AngloGold Ashanti's geotechnical team will first run more trials of rockbolt extraction in further areas to substantiate associated findings more broadly for a bigger variety of scenarios and existing support designs. This will be followed by a more comprehensive review to assess opportunities for ground support design improvement. Other ground support design improvement opportunities include trialling or tracking of existing different installed ground support system designs in equivalent ground condition drives to compare their performance. If one particular system design performs better, then it can be adopted as the one to go forward with in all applicable new mining areas.

3 Conclusion

The authors have presented a novel methodology to automatically extract and track specific spatial characteristics of the majority of rockbolts contained in typical LiDAR scans collected in underground drives. Aggregating this bolt and plate deformation data into representative graphs and 3D data allows for meaningful assessment of ground support degradation and remaining capacity. The case study presented an opportunity to determine ground support deformation at failure as failures occurred and were tracked through LiDAR scans and subsequent automated processing. Cuiabá's and AngloGold Ashanti's geotechnical team will use this data as the first input into a larger study to determine quantified deformation triggers for preventative rehabilitation, and depending on the outcomes of further studies, on possible ground support design modifications if applicable.

Acknowledgement

The authors would like to acknowledge Jony Alves and Felipe Franco responsible for scanning the galleries, all completed with a very high degree of accuracy in georeferencing that allows for equally accurate deformation tracking. Thanks also go to Marcelo Fernandes from the mine topography team for helping with the implementation of the process.

Disclaimer

Jochen Franke and Carlos Gonzalez are employees of Caroni Geospatial Pty Ltd, the developer and commercial provider of the VoidMapper software used in this case study. AngloGold Ashanti is a client of Caroni Geospatial. All technical findings and conclusions presented in this paper reflect the independent assessment of the Cuiabá Mine geotechnical team.

References

Fernandes, R, Endo, I, Pereira, R & Souza, J 2016, 'Geology and structural evolution of the cuiabá gold deposit: new perspectives for mineral exploration', *VII Simpósio Brasileiro de Exploração Mineral*, SIMEXMIN, Ouro Preto.

Franke, J & Gonzalez, C 2022, 'Automated omission-free geotechnical deformation monitoring – a new method deployable by non-specialists', *Proceedings of Ausrock Conference 2022*, Australasian Institute of Mining and Metallurgy, Melbourne, pp. 15–17.

Franke, J & Gonzalez, C 2023, 'Automated ground support deformation monitoring: a novel method with new opportunities for geotechnical engineers', in J Wesseloo (ed.), *Ground Support 2023: Proceedings of the 10th International Conference on Ground Support in Mining*, Australian Centre for Geomechanics, Perth, pp. 75–90, https://doi.org/10.36487/ACG_repo/2325_04

Franke, J & Gonzalez, C 2024, 'Automated ground and support deformation monitoring: a novel method with expanded features for geotechnical engineers', in P Andrieux & D Cumming-Potvin (eds), *Deep Mining 2024: Proceedings of the 10th International Conference on Deep and High Stress Mining*, Australian Centre for Geomechanics, Perth, pp. 429–444, https://doi.org/10.36487/ACG_repo/2465_23

Franke, J & Gonzalez, C 2026, *VoidMapper*, version 5, computer software, Caroni Geospatial, Perth, https://voidmapper.com.au/

Rodrigues, L, de Oliveira, C & Friedrich, G 2007, 'The Archean BIF-hosted Cuiabá Gold deposit, Quadrilátero Ferrífero, Minas Gerais, Brazil', *Ore Geology Reviews*, vol. 32, pp. 543–570.